Stability of equilibrium states in finite samples of smectic C* liquid crystals

2005 J. Phys. A: Math. Gen. 38 1853

(http://iopscience.iop.org/0305-4470/38/9/003)

INSTITUTE OF PHYSICS PUBLISHING JOURNAL OF PHYSICS A: MATHEMATICAL AND GENERAL

J. Phys. A: Math. Gen. **38** (2005) 1853–1873 doi:10.1088/0305-4470/38/9/003

Stability of equilibrium states in finite samples of smectic C* liquid crystals

I W Stewart

Department of Mathematics, University of Strathclyde, Livingstone Tower, 26 Richmond Street, Glasgow G1 1XH, UK

E-mail: i.w.stewart@strath.ac.uk

Received 9 September 2004, in final form 13 January 2005
Published 16 February 2005
Online at stacks.iop.org/JPhysA/38/1853

Abstract

Equilibrium solutions for a sample of ferroelectric smectic C (SmC*) liquid crystal in the 'bookshelf' geometry under the influence of a tilted electric field will be presented. A linear stability criterion is identified and used to confirm stability for typical materials possessing either positive or negative dielectric anisotropy. The theoretical response times for perturbations to the equilibrium solutions are calculated numerically and found to be consistent with estimates for response times in ferroelectric smectic C liquid crystals reported elsewhere in the literature for non-tilted fields.

PACS numbers: 61.30.−v, 61.30.Dk

1. Introduction

Smectic liquid crystals are anisotropic fluids consisting of rod-like molecules which are arranged in equidistant layers. These molecules have a common preferred local average direction within each layer and the average orientation of their long molecular axes is described by the unit vector **n**, usually called the director. In non-chiral smectic C liquid crystals (SmC) the director is tilted relative to the layer normal **a** at an angle θ, called the smectic tilt angle or smectic cone angle, as depicted in figure 1(a). The tilt angle θ is generally temperature dependent; nevertheless, in this paper we shall assume isothermal conditions and suppose that θ is a fixed constant angle. Under this assumption, it follows that **n** is constrained to rotate around the surface of a fictitious cone as pictured in figure 1(b). It is an accepted practice [1] to introduce the vector **c** as the unit orthogonal projection of **n** onto the smectic planes as shown in figure 1(b), from which it is then seen that

$$\mathbf{n} = \mathbf{a}\cos\theta + \mathbf{c}\sin\theta. \tag{1.1}$$

Knowledge of **a** and **c** completely determines the alignment of the director **n**. Ferroelectric smectic C liquid crystals (SmC*) are chiral forms of SmC liquid crystals: in addition to the

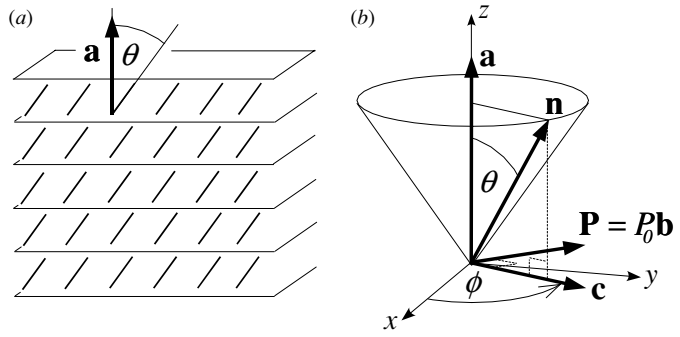

Figure 1. (*a*) A planar layered sample of SmC liquid crystal. The short bold lines represent the alignment of the director **n**, which is always tilted at an angle θ to the layer normal **a**. (*b*) The vector **c** represents the unit orthogonal projection of **n** onto the smectic planes. The angle ϕ is used to describe the orientation of **c** within the xy-plane. In ferroelectric SmC* there is also a spontaneous polarization vector $\mathbf{P} = P_0\mathbf{b}$ where $\mathbf{b} = \mathbf{a} \times \mathbf{c}$. In the isothermal situation θ is constant and in both SmC and SmC* the director **n** is then constrained to rotate around the surface of a fictitious cone.

aforementioned properties of SmC they posses a spontaneous polarization vector **P** which is normal to both **a** and **n**. It then proves convenient to introduce the vector $\mathbf{b} = \mathbf{a} \times \mathbf{c}$ in order to describe **P** by

$$\mathbf{P} = P_0\mathbf{b}, \qquad P_0 = |\mathbf{P}|. \tag{1.2}$$

In SmC* liquid crystals the spontaneous polarization **P**, and therefore the vector **c**, exhibits an inherent rotation within the xy-plane as an observer travels along the z-axis in figure 1(*b*). This generates the helical structure of these chiral materials. If the smectic layers are fixed in parallel planes then the orientation angle ϕ of **c** measured relative to the x-axis enables a full description of the orientation of the director **n**, by (1.1), and the spontaneous polarization **P**, since it always lies in the xy-plane orthogonal to **c**. Following the convention of Lagerwall and Dahl [2], **P** as defined in (1.2) is called positive. Negative polarization is also known to occur in physical samples, in which case we can write $\mathbf{P} = -P_0\mathbf{b}$, with $P_0 > 0$. We shall assume positive polarization below: the case for negative polarization can be considered analogously. Further background details on SmC and SmC* liquid crystals may be found in [1, 3, 4].

It is well known that externally applied electric fields influence the orientation of **n**. It is the aim of this paper to obtain equilibrium solutions for a sample of SmC* in the standard 'bookshelf' geometry when the director has been anchored at different orientations on each boundary plate and an electric field is applied across the sample at an angle α to the normal of the plates. For the case when the electric field is perpendicular to the plates, Maclennan *et al* [5] considered the dynamics of the director in SmC* while Anderson and Stewart [6, 7] obtained static equilibrium solutions and considered their stability. When the electric field is tilted relative to the plane of the smectic layers then the structure of the equilibrium configurations changes. Experimental results and some elementary dynamics were reported by Abdulhalim *et al* [8, 9] when the smectic layers were tilted between boundary plates across which an electric field was applied. In these papers a model dynamic equation was given and this equation will be of the same form and structure as that to be discussed below. When the field is tilted relative to the layers there are essentially three sinusoidal contributions to the nonlinear terms appearing in the dynamic equation; when the tilt of the field is zero, there are only two sinusoidal contributions. Some exact solutions are known for the dynamic equation in the latter case and will be mentioned below, but no exact solutions are known in the former.

In section 2 the dynamic theory and a mathematical description of the problem will be presented. We shall obtain equilibrium solutions numerically in section 3 for non-zero tilted electric fields when the elastic constants are set equal. The stability of these non-constant static solutions will be investigated in section 4. For a typical SmC* material we shall establish stability via a quite general stability criterion in section 4.1, given by (4.14). This consequently encourages a search in section 4.2 for the explicit dynamic response to perturbations of these equilibrium solutions. The characteristic response times for such perturbations in a typical material, for various magnitudes of electric field, will be derived numerically via the Ritz method for obtaining the eigenvalues of a regular Sturm–Liouville boundary value problem. These theoretical response times for high magnitude fields, presented in figure 6, are within the range of characteristic response times reported for SmC* liquid crystals when switching phenomena are considered [3, 10]. Section 5 considers the problem when the elastic constants are not equal; for brevity, attention is restricted to the case where the dielectric anisotropy is positive. The effects of anisotropy in the elastic constants upon the equilibrium solutions, and perturbations to them, are shown in figures 7 and 8. The paper closes in section 6 with a discussion of the results.

2. Dynamic theory and description of the problem

The dynamic theory of Leslie *et al* [11] will be employed to obtain the governing static and dynamic equations that will describe the orientation of the vector **c** within the smectic planes. A brief summary of the parts of this theory that will be applicable will now be given before we go on to discuss the geometrical set-up of the problem to be investigated and the consequent dynamic equation for describing the reorientation of the vector **c** under the influence of a tilted electric field.

2.1. Dynamic theory

The smectic layer normal **a** and the vector **c** introduced in figure 1 must satisfy the constraints

$$\mathbf{a}\cdot\mathbf{a} = \mathbf{c}\cdot\mathbf{c} = 1, \qquad \mathbf{a}\cdot\mathbf{c} = 0. \tag{2.1}$$

If the sample is assumed to have no dislocations, as will be supposed here, then the layer normal **a** must additionally fulfil the requirement [12]

$$\nabla\times\mathbf{a} = \mathbf{0}. \tag{2.2}$$

The bulk elastic energy density (integrand) for SmC* liquid crystals may be written in Cartesian component form as [4] (see also [13, 14] for alternative formulations)

$$\begin{aligned} w_{\text{elas}} = {} & \tfrac{1}{2}A_{21}(a_{i,i})^2 + \tfrac{1}{2}(B_2 - B_3)(c_{i,i})^2 + \tfrac{1}{2}(B_1 - B_3)c_{i,j}c_jc_{i,k}c_k + \tfrac{1}{2}B_3c_{i,j}c_{i,j} \\ & + \tfrac{1}{2}(A_{12} + A_{21} + 2A_{11} - B_1 + B_3)(c_ia_{i,j}c_j)^2 \\ & - \left(A_{11} + A_{21} + \tfrac{1}{2}B_3\right)a_{i,i}(c_ja_{j,k}c_k) + B_{13}c_{i,j}c_jc_{i,k}a_k + (C_1 + C_2)c_{i,i}(c_ja_{j,k}c_k) \\ & - C_2a_{i,i}c_{j,j} + 2A_{11}\delta\epsilon_{ipk}a_pc_kc_{j,i}a_j - B_3q\epsilon_{ipk}a_pc_kc_{i,j}a_j, \end{aligned} \tag{2.3}$$

where repeated indexes are summed from 1 to 3 and a comma denotes partial differentiation with respect to the variable it precedes. There are nine elastic constants and they are known to obey the inequalities

$$A_{12},\, A_{21},\, B_1,\, B_2,\, B_3 \geqslant 0, \qquad A_{12}A_{21} - A_{11}^2 \geqslant 0, \tag{2.4}$$

$$B_1B_3 - B_{13}^2 \geqslant 0, \qquad B_2A_{12} - C_1^2 \geqslant 0, \qquad B_2A_{21} - C_2^2 \geqslant 0. \tag{2.5}$$

A physical interpretation of these constants may be found elsewhere [4, 15]; it is worth recording that the A_i constants relate to bending of the smectic layers, the B_i refer to various distortions of the vector **c** and the C_i are coupling constants related to various layer deformations that are linked with distortions of **c**. The constants B_1 and B_2 are particularly relevant to the discussion below and are related to the reorientation of **c** within the smectic planes. The parameter $q > 0$ is a wave number related to the chirality of the SmC* phase while δ is generally accepted as being zero in undistorted planar layers of smectic [1, 14].

In SmC* liquid crystals there are contributions to the electric energy density given by [1, 3, 4]

$$w_{\text{elec}} = -\mathbf{P}\cdot\mathbf{E} - \tfrac{1}{2}\epsilon_0\epsilon_a(\mathbf{n}\cdot\mathbf{E})^2, \tag{2.6}$$

where **E** is the electric field, ϵ_0 is the permittivity of free space and ϵ_a is the (unitless) dielectric anisotropy, which may be positive or negative. The director prefers to align itself parallel to the field when $\epsilon_a > 0$ and perpendicular to the field when $\epsilon_a < 0$. The first contribution on the right-hand side of (2.6) is minimized when **P** (in the direction of **b**) is parallel to **E**. It is well known that the spontaneous polarization has a dominant influence for electric fields of small magnitude and that the dielectric contribution dominates at high magnitude fields.

The total energy density w for SmC* is the sum of the elastic and electric energies, which leads to

$$w = w_{\text{elas}} + w_{\text{elec}}, \tag{2.7}$$

with the total energy being given by

$$W = \int_V w\,\mathrm{d}V, \tag{2.8}$$

where V is the volume of the sample.

The dynamic equations when flow is neglected, as it will be in this paper, are generally split into two coupled systems of 'a-equations' and 'c-equations'. In the problem to be described below in section 2.2 we shall consider a sample of SmC* which has a fixed system of parallel planar aligned smectic layers. In these circumstances the layer normal **a** is a constant vector and therefore the a-equations need not concern us here in this brief analysis. Only the c-equations will be of relevance under these assumptions and they may be written as [4, 11]

$$\Pi_i^c + \tilde{g}_i^c + \mu a_i + \tau c_i = 0, \qquad i = 1, 2, 3, \tag{2.9}$$

where,

$$\Pi_i^c = \left(\frac{\partial w}{\partial c_{i,j}}\right)_{,j} - \frac{\partial w}{\partial c_i}, \tag{2.10}$$

and

$$\tilde{g}_i^c = -2\lambda_5\frac{\partial c_i}{\partial t}. \tag{2.11}$$

The parameter λ_5 is known to be a positive viscosity coefficient related to the rotation of the director **n** around the fictitious cone illustrated in figure 1(b) [4, 11]. The scalar functions μ and τ are Lagrange multipliers which arise from the constraints that **a** and **c** are mutually orthogonal unit vectors. These multipliers may be found by taking the scalar product of equations (2.9) with **a** and **c**. The dynamic equations are then given by solutions to (2.9) once the Lagrange multipliers have been found or eliminated. The static equilibrium equations are provided by time-independent solutions to (2.9).

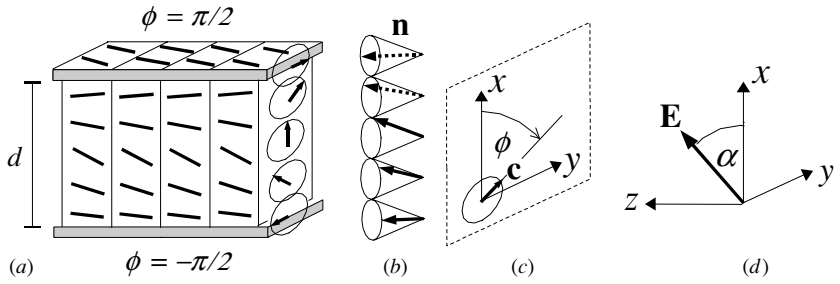

Figure 2. (*a*) The 'bookshelf' geometry for SmC* liquid crystals. The parallel smectic layers are perpendicular to the boundary plates at $x = 0$ and $x = d$. For simplicity, the director is fixed at the boundaries so that the vector **c** is parallel to the plates at both boundaries but in opposing directions. The possible orientation of **c** across the sample is shown on the right-hand side. (*b*) A schematic representation of **n** across the sample. (*c*) The orientation angle ϕ of **c** within the xy-plane. (*d*) The coordinate system showing the electric field **E** being applied across the boundary plates at an angle α to the plane of the smectic layers.

2.2. Description of the problem

Consider a sample of planar layers of SmC* liquid crystal in the bookshelf geometry having depth d as illustrated in figure 2(*a*). An electric field **E** is applied across the plates at an angle α to the plane of the smectic layers as shown in figure 2(*d*). The vector **c** is described by the phase angle $\phi(x, t)$ as depicted in figure 2(*c*). The director is fixed at the top and bottom plates so that $\phi(0, t) = -\pi/2$ and $\phi(d, t) = \pi/2, t \geqslant 0$; this gives a total reorientation through π radians as ϕ varies between the plates. The orientation of **c** is pictured schematically on the right-hand side of figure 2(*a*), showing the orientation of **n** around the fictitious cone as shown in figure 2(*b*). Under this geometry and the description in figure 1(*b*) we can write

$$\mathbf{a} = (0, 0, 1), \tag{2.12}$$

$$\mathbf{c} = (\cos\phi(x, t), \sin\phi(x, t), 0), \tag{2.13}$$

$$\mathbf{b} = (-\sin\phi(x, t), \cos\phi(x, t), 0), \tag{2.14}$$

$$\mathbf{P} = P_0\mathbf{b}, \tag{2.15}$$

$$\mathbf{E} = E(\cos\alpha, 0, \sin\alpha), \tag{2.16}$$

where the dependence of the orientation angle ϕ upon x and t only is supposed and E is the magnitude of the electric field. A detailed analysis of the electric energy w_{elec} in (2.6) for the case considered in equations (2.12) to (2.16) has been discussed recently by Stewart and Momoniat [16].

We must first eliminate or identify the Lagrange multipliers. Taking the scalar product of equations (2.9) with the forms for **a** and **c** given by equations (2.12) and (2.13) gives, respectively,

$$\mu = -\Pi_3^c, \qquad \tau = -\Pi_i^c c_i, \tag{2.17}$$

upon observing that $\tilde{g}_i^c c_i$ and $\tilde{g}_i^c a_i$ are both identically zero because $\mathbf{c}\cdot\mathbf{c} = 1$ and **a** is a constant vector. The third of the c-equations ($i = 3$) in (2.9) is automatically satisfied for these Lagrange multipliers, and therefore the remaining c-equations may be written as

$$\Pi_1^c + \tilde{g}_1^c + \tau\cos\phi = 0, \tag{2.18}$$

$$\Pi_2^c + \tilde{g}_2^c + \tau \sin\phi = 0. \tag{2.19}$$

Multiplying (2.18) by $\sin\phi$ and (2.19) by $\cos\phi$ and subtracting the resulting equations then eliminates τ and yields the governing dynamic equation

$$\Pi_1^c \sin\phi - \Pi_2^c \cos\phi + \tilde{g}_1^c \sin\phi - \tilde{g}_2^c \cos\phi = 0. \tag{2.20}$$

We do not require to calculate Π_3^c for our purposes. The quantities $\tilde{g}_1^c$, $\tilde{g}_2^c$, Π_1^c and Π_2^c can be calculated explicitly from equations (1.1), (2.3), (2.6), (2.7) and (2.10) to (2.16) to find, after some straightforward manipulations,

$$\tilde{g}_1^c = 2\lambda_5 \sin\phi \frac{\partial\phi}{\partial t}, \tag{2.21}$$

$$\tilde{g}_2^c = -2\lambda_5 \cos\phi \frac{\partial\phi}{\partial t}, \tag{2.22}$$

$$\Pi_1^c = -B_2 \left[\cos\phi \left(\frac{\partial\phi}{\partial x} \right)^2 + \sin\phi \frac{\partial^2\phi}{\partial x^2} \right] + \epsilon_a \epsilon_0 E^2 \sin\theta \cos\alpha \, (\sin\alpha \cos\theta + \cos\alpha \sin\theta \cos\phi), \tag{2.23}$$

$$\Pi_2^c = -B_1 \left[\sin\phi \left(\frac{\partial\phi}{\partial x} \right)^2 - \cos\phi \frac{\partial^2\phi}{\partial x^2} \right] - P_0 E \cos\alpha, \tag{2.24}$$

where θ is the constant smectic tilt angle. Inserting these results into (2.20) finally reveals the governing dynamic equation

$$2\lambda_5 \frac{\partial\phi}{\partial t} = [B_1 \cos^2\phi + B_2 \sin^2\phi] \frac{\partial^2\phi}{\partial x^2} + (B_2 - B_1) \left(\frac{\partial\phi}{\partial x} \right)^2 \sin\phi \cos\phi - P_0 E \cos\alpha \cos\phi - \epsilon_0 \epsilon_a E^2 \cos\alpha \sin\alpha \cos\theta \sin\theta \sin\phi - \epsilon_0 \epsilon_a E^2 \cos^2\alpha \sin^2\theta \sin\phi \cos\phi. \tag{2.25}$$

Note that the wave number q does not enter the equilibrium equations; it does, nevertheless, affect the value of the total energy W.

2.2.1. One-constant approximation. A qualitative analysis of the dynamic equation (2.25) is made more tractable by making the one-constant approximation $B_1 = B_2 \equiv B$. In this case the dynamic equation for $\phi(x, t)$ reduces to

$$2\lambda_5 \frac{\partial\phi}{\partial t} = B \frac{\partial^2\phi}{\partial x^2} - P_0 E \cos\alpha \cos\phi - \epsilon_0 \epsilon_a E^2 \cos\alpha \sin\alpha \cos\theta \sin\theta \sin\phi - \epsilon_0 \epsilon_a E^2 \cos^2\alpha \sin^2\theta \sin\phi \cos\phi. \tag{2.26}$$

The time-independent equilibrium solutions $\phi(x)$ satisfy the equation

$$B \frac{\partial^2\phi}{\partial x^2} = P_0 E \cos\alpha \cos\phi + \epsilon_0 \epsilon_a E^2 \cos\alpha \sin\alpha \cos\theta \sin\theta \sin\phi + \epsilon_0 \epsilon_a E^2 \cos^2\alpha \sin^2\theta \sin\phi \cos\phi. \tag{2.27}$$

We shall be presenting solutions to the equilibrium equation (2.27) in section 3 and investigating their stability in section 4 by means of the dynamic equation (2.26), where ϕ satisfies the strong anchoring boundary conditions

$$\phi(0, t) = -\frac{\pi}{2}, \qquad \phi(d, t) = \frac{\pi}{2}, \qquad t \geqslant 0. \tag{2.28}$$

These conditions reflect a net change in reorientation of the vector $\mathbf{c}$ at the boundaries of π radians as ϕ varies between the boundary plates, as shown in figure 2. Different boundary

conditions for ϕ can be accommodated by the procedures outlined below: the above boundary conditions were chosen in order to enable qualitative observations to be made by identifying simple constant equilibrium solutions that ϕ may attempt to achieve in the bulk of the sample.

Guided by the results obtained from (2.26) and (2.27), equation (2.25) for the case of different elastic constants will be investigated in section 5 where it will be shown that the effect upon equilibrium solutions due to anisotropy in the elastic constants is more pronounced in low magnitude field regimes.

3. Solutions for the one-constant approximation

Numerical solutions to the static equilibrium equation (2.27) for the bookshelf geometry problem described via figure 2 in section 2 will now be presented. It is convenient to assume unit lengths in the y and z directions and to normalize the sample depth in the x direction by setting $X = x/d$ and then, to ease notation, replace X by x with $0 \leqslant x \leqslant 1$; the notational context should be clear and ought not to lead to confusion. The equilibrium equation (2.27) may then be written as

$$\frac{\mathrm{d}^2\phi}{\mathrm{d}x^2} = aE^2 \sin\phi\cos\phi + bE\cos\phi + cE^2\sin\phi, \tag{3.1}$$

where

$$a = \epsilon_0\epsilon_a d^2 B^{-1}\cos^2\alpha\sin^2\theta, \tag{3.2}$$

$$b = P_0 d^2 B^{-1}\cos\alpha, \tag{3.3}$$

$$c = \epsilon_0\epsilon_a d^2 B^{-1}\cos\alpha\sin\alpha\cos\theta\sin\theta, \tag{3.4}$$

with boundary conditions

$$\phi(0) = -\frac{\pi}{2}, \qquad \phi(1) = \frac{\pi}{2}, \tag{3.5}$$

which correspond to a 'π-twist' cell. Observe that the governing equation (3.1) is invariant to the simultaneous changes in sign of E and ϕ while the boundary conditions are not invariant: a change in the sign of E will alter the solutions, as will be seen in the figures that are presented below for both positive and negative fields. Solutions for both signs of E are considered because a change in sign is of importance when considering the switching of liquid crystal cells. Nevertheless, it is seen from (3.1) and (3.5) that the solutions obey the symmetry condition $\phi(x) \mapsto -\phi(1-x)$ as the sign of E is changed. This observation means that when examining stability in sections 4 and 5 we can can restrict attention to the case for $E > 0$ because the situation for $E < 0$ is analogously found via symmetry: the stability criterion developed in section 4.1 will be equally valid for either sign of E.

One reason for selecting the boundary conditions (3.5) is that if $\alpha = 0$ then $\phi = \pm\pi/2$ are the natural constant equilibrium solutions to (3.1); they are also the naturally preferred constant equilibria when $|E| \ll 1$. Of course, these constant solutions cannot match the given boundary conditions, but they can be considered as possible preferential states for the system in the bulk of the sample away from the boundaries. Further, when $\alpha = 0$, one of these constant equilibria becomes preferred to the other as the magnitude of the electric field increases. It is this 'competition' between possible constant equilibria and boundary conditions that will influence the structure of the non-constant equilibrium solutions. Note also that for $|E| \gg 1$ the dominating terms in equation (3.1) are those with the coefficients a and c and that $\phi = 0$ and $\phi = \pm\pi$ then become possible candidates as constant equilibrium solutions to which ϕ

may be attracted in the bulk of the sample. It is expected that ϕ will attempt to achieve a compromise between the boundary conditions and the states $\pm\pi$ for large magnitude fields when $\alpha \geqslant 0$.

Qualitatively, the results will be similar for various sample depths d, and therefore we proceed by fixing typical values for the physical parameters and only allow the electric field to change in order to see its influence upon ϕ as it varies across the sample. For typical values we set [3, 4]

$$B = 5 \times 10^{-12}\ \mathrm{N}, \qquad P_0 = 80\ \mu\mathrm{C\ m^{-2}}, \qquad \theta = 22^\circ, \qquad \alpha = 5^\circ, \qquad d = 10\ \mu\mathrm{m}, \tag{3.6}$$

with $\epsilon_0 = 8.854 \times 10^{-12}\ \mathrm{F\ m^{-1}}$ being the usual value for the permittivity of free space. It is known that the dielectric anisotropy of many liquid crystals lies approximately in the range $|\epsilon_a| \lesssim 10$ [17], with many SmC* liquid crystals being known to possess negative dielectric anisotropy ϵ_a around -3 to -0.5. We shall select $\epsilon_a = -2$ and $\epsilon_a = 2$ as representative values in the following examples.

Case (i) $\epsilon_a = 2$. We begin with the case for positive dielectric anisotropy $\epsilon_a = 2$. Numerical solutions to equation (3.1) with the boundary conditions (3.5) and physical parameters (3.6) have been obtained using the dsolve routine contained in the software package Maple 8 [18]. The spontaneous polarization contribution is linear in E while the dielectric contributions are quadratic and therefore solutions have been derived for both positive and negative electric fields. Figure 3(a) shows the solution $\phi(x)$, $0 \leqslant x \leqslant 1$, for $E > 0$ as the field magnitude increases and figure 3(b) shows the situation for $E < 0$. When there is no field there is a linear solution for ϕ given by $\phi(x) = (2x - 1)\pi/2$. As E increases above zero, it is seen in figure 3(a) that ϕ initially has a tendency, in the bulk of the sample, to approach the constant solution $\phi = -\pi/2$, a possibility that was identified above for small magnitude fields. This behaviour arises because the effect of the spontaneous polarization, characterized by the contribution with coefficient b in equation (3.1), will be more influential for small magnitude fields. However, as E increases further, the dielectric terms with coefficients a and c begin to dominate and ϕ then attempts to approach a constant solution in the bulk that is a compromise between the boundary states $\phi = \pm\pi/2$ and the constant state $\phi = 0$, this latter state having been identified earlier as being close to a possible preferred equilibrium in the bulk for high magnitude fields.

The situation for $E < 0$ is shown in figure 3(b). Initially, ϕ attempts to approach $\pi/2$ as $|E|$ increases above zero. In an analogous way to that discussed above for $E > 0$, when $|E|$ increases further ϕ again attempts to approach a constant solution in the bulk of the sample that is a compromise between the boundary states $\pm\pi/2$ and the constant state $\phi = 0$.

Case (ii) $\epsilon_a = -2$. When the dielectric anisotropy $\epsilon_a = -2$ the numerical solutions for $\phi(x)$ have similar behaviour to those when $\epsilon_a = 2$, in the sense that for low magnitude fields ϕ tries to approach the states $\phi = -\pi/2$ when $E > 0$ and $\phi = \pi/2$ when $E < 0$. Such solutions are shown in figure 4. However, the profiles in figure 4 differ from those in figure 3 when $|E|$ increases such that the dielectric terms dominate the behaviour. For large $E > 0$ the solution ϕ attempts to achieve a compromised constant equilibrium state in the bulk that is less than $-\pi/2$, as can be seen in figure 4(a): the compromised state lies between $-\pi/2$ and the preferred bulk equilibrium state $-\pi$, identified in the first paragraph of this section. This is in contrast to the case for $\epsilon_a = 2$ where ϕ attempts to reach a constant equilibrium state in the bulk that is between $-\pi/2$ and $\pi/2$ for high magnitude fields. An analogous situation occurs for $E < 0$, as is clear from figure 4(b), where ϕ seeks a constant equilibrium solution that lies between $\pi/2$ and the preferred bulk equilibrium π when $|E|$ is large.

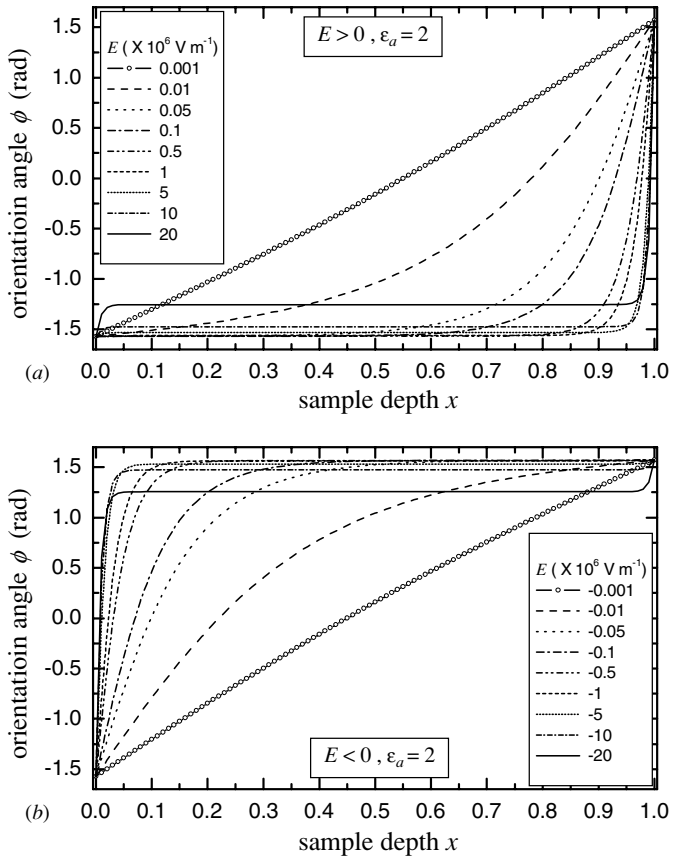

Figure 3. Numerical solutions to equation (3.1) with boundary conditions (3.5) for the parameters (3.6) when $\epsilon_a = 2$. (*a*) $E > 0$. (*b*) $E < 0$.

Remark. In both cases (i) and (ii) the constant states that the equilibrium solutions $\phi(x)$ attempt to reach in the bulk can be approximated numerically. For example they can be computed for any tilted field angle α for each value of E by setting the right-hand side of equation (3.1) to zero and solving for its roots in ϕ. In all cases, irrespective of the value of α, the dominant behaviour is dictated by the spontaneous polarization at low magnitude electric fields and the dielectric contributions at high magnitude fields.

4. Stability in the one-constant approximation

The stability of the equilibrium solutions derived above will now be investigated. This is accomplished by considering a small perturbation w to these solutions where w vanishes at the boundaries and depends on space and time. If we introduce the rescaled time T by

$$T = \frac{t}{\tau_d}, \qquad \text{where} \quad \tau_d = 2\frac{\lambda_5 d^2}{B}, \tag{4.1}$$

then, recalling that we have normalized x at the beginning of section 3, the dynamic equation (2.26) can be written, in the notation of equations (3.1) to (3.4), as

$$\frac{\partial \phi}{\partial T} = \frac{\partial^2 \phi}{\partial x^2} - aE^2 \sin\phi\cos\phi - bE\cos\phi - cE^2\sin\phi. \tag{4.2}$$

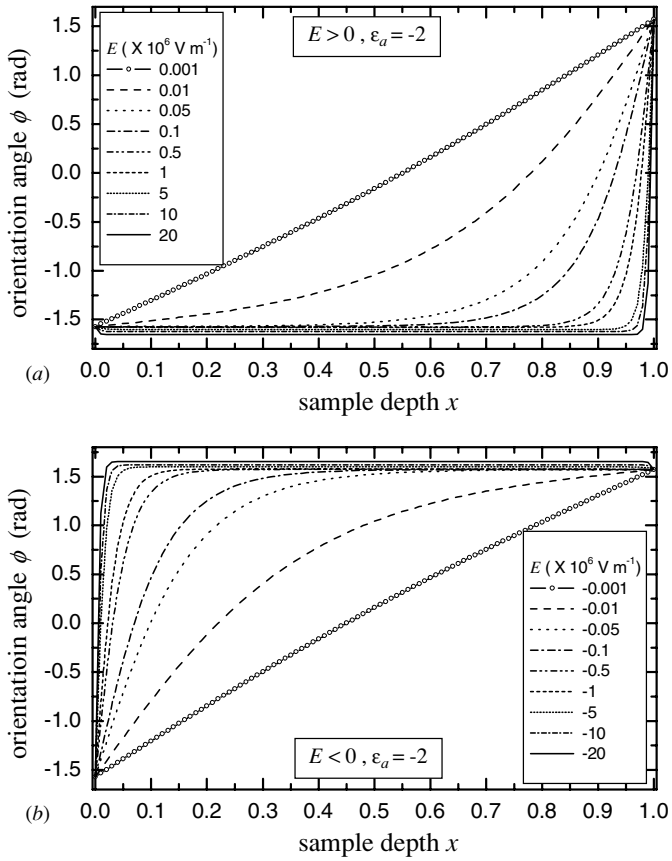

Figure 4. Numerical solutions to equation (3.1) with boundary conditions (3.5) for the parameters (3.6) when $\epsilon_a = -2$. (*a*) $E > 0$. (*b*) $E < 0$.

Let $\overline{\phi}(x)$ denote any equilibrium solution to equation (3.1) and consider

$$\phi(x, T) = \overline{\phi}(x) + w(x, T), \quad |w| \ll 1. \tag{4.3}$$

Substituting this form for $\phi(x, T)$ into (4.2) and expanding the equation to first order of magnitude in w leads to the governing dynamic equation for the perturbation w to $\overline{\phi}$. Recalling that $\overline{\phi}(x)$ must fulfil (3.1), we find that the relevant dynamic equation which governs the linear stability of our problem is given by

$$\frac{\partial w}{\partial T} = \frac{\partial^2 w}{\partial x^2} - [aE^2 \cos(2\overline{\phi}) - bE \sin\overline{\phi} + cE^2 \cos\overline{\phi}]w. \tag{4.4}$$

Now suppose

$$w(x, T) = \mathrm{e}^{-\lambda T} v(x), \qquad v(0) = v(1) = 0. \tag{4.5}$$

If it can be shown that $\lambda > 0$ then we can conclude that $w(x, T) \to 0$ as $T \to \infty$ so that perturbations decay to zero, which indicates that the equilibrium solution $\overline{\phi}(x)$ is asymptotically stable. Moreover, if we can determine the values λ for given electric field values E, then we can establish more detailed stability results and find the characteristic

response times for such perturbations. With this idea in mind, we proceed by inserting (4.5) into (4.4) to yield the regular Sturm–Liouville boundary value problem

$$\frac{\mathrm{d}^2 v}{\mathrm{d}x^2} + [\lambda - q(x)]v(x) = 0, \qquad v(0) = v(1) = 0, \tag{4.6}$$

where

$$q(x) = aE^2 \cos(2\overline{\phi}(x)) - bE \sin\overline{\phi}(x) + cE^2 \cos\overline{\phi}(x). \tag{4.7}$$

Any function $v(x)$ that is not identically zero and satisfies (4.6), including its boundary conditions, is called an eigenfunction corresponding to the eigenvalue λ. It is well known [19] that for a regular Sturm–Liouville problem there are infinitely many discrete eigenvalues $\lambda_1, \lambda_2, \lambda_3, \ldots$, which can be ordered such that $\lambda_1 < \lambda_2 < \lambda_3 < \ldots$. It therefore follows that if the least eigenvalue λ_1 is positive then all the eigenvalues are positive and then all perturbations will decay to zero on account of them being of the form stated in equation (4.5). The question of stability then reduces to identifying whether or not the least eigenvalue λ_1 is positive.

It is also known [19] that the positivity of the eigenvalues of a regular Sturm–Liouville problem (4.6) is closely related to the behaviour of the function $q(x)$. For example, if $q(x)$ is continuous and strictly positive then the eigenvalues are strictly positive. However, in the problem considered here, the equilibrium solutions $\overline{\phi}(x)$ satisfy $\overline{\phi}(0) = -\pi/2$ and $\overline{\phi}(1) = \pi/2$ which force, via (4.7),

$$q(0) = -aE^2 + bE, \qquad q(1) = -aE^2 - bE, \tag{4.8}$$

and so, in general, $q(x)$ cannot always be strictly positive on the interval [0, 1]. There are a number ways of overcoming this problem in dealing with the sign of q. One key method is to formulate the problem in an integral form and employ the Hardy inequality to ensure positivity of λ, as will be seen in section 4.1 below. A variant of this inequality was used in [7] for a case that was mathematically equivalent to setting $\alpha = 0$ (equivalent to setting $c = 0$), but it could only be used after certain limitations on the magnitude of electric field were imposed. We shall remove the restrictions on both α and E by using a particularly appropriate version of the Hardy inequality.

4.1. A stability criterion

It is possible to multiply the differential equation in (4.6) by v and integrate with respect to x over the interval [0, 1]. Applying the boundary conditions on v after an obvious integration by parts on the term that involves the second derivative then leads to the relation

$$\int_0^1 \left[\left(\frac{\mathrm{d}v}{\mathrm{d}x} \right)^2 + q(x)v(x)^2 \right] \mathrm{d}x = \lambda \int_0^1 v^2(x)\, \mathrm{d}x, \tag{4.9}$$

a form that is familiar for regular Sturm–Liouville problems [19]. Clearly, if we define

$$I(v) \equiv \int_0^1 \left[\left(\frac{\mathrm{d}v}{\mathrm{d}x} \right)^2 + q(x)v(x)^2 \right] \mathrm{d}x \tag{4.10}$$

then it is seen from (4.9) that $\lambda \geqslant 0$ if we can establish that $I(v) \geqslant 0$ whenever v is not identically the zero function. Strict positivity of $I(v)$ will then show that $\lambda > 0$, which indicates that the perturbation is asymptotically stable. The positivity of $I(v)$ cannot be determined in a trivial way since $q(x)$ can take negative and positive values. This leads us to a discussion of the Hardy inequality.

For any smooth function v on the interval $[0, 1]$ such that $\mathrm{d}v/\mathrm{d}x \in L^2(0, 1)$ and $v(0) = v(1) = 0$, one variant of the Hardy inequality states that (cf [20, p 105])

$$\int_0^1 \left(\frac{\mathrm{d}v}{\mathrm{d}x}\right)^2 \mathrm{d}x \geqslant \frac{1}{4}\int_0^1 \frac{v^2(x)}{m^2(x)}\,\mathrm{d}x, \tag{4.11}$$

where

$$m(x) = \min\{x, 1 - x\}, \qquad 0 < x < 1. \tag{4.12}$$

Under such assumptions on the function v, this inequality can be applied to $I(v)$ to find that

$$I(v) \geqslant \frac{1}{4}\int_0^1 \frac{1}{m^2(x)}[1 + 4m^2(x)q(x)]v^2(x)\,\mathrm{d}x. \tag{4.13}$$

Therefore, $I(v)$, and consequently λ, will be non-negative provided

$$r(x) \equiv 1 + 4m^2(x)q(x) \geqslant 0, \qquad \text{for all} \quad 0 \leqslant x \leqslant 1. \tag{4.14}$$

Perturbations will be stable if the criterion in equation (4.14) is satisfied. Moreover, provided v is an eigenfunction (and is therefore not identically zero), perturbations will be asymptotically stable if the inequality in (4.14) is strict, i.e. $r(x) > 0$ for all $0 < x < 1$. Thus the positivity of $r(x)$, which only involves knowledge of $q(x)$ (which is itself based upon the known equilibrium solution $\overline{\phi}(x)$), provides a stability criterion for perturbations.

The numerical solutions displayed in figures 3 and 4 can be inserted into the criterion (4.14) to determine the positivity of $r(x)$. The results are shown in figure 5 for $\epsilon_a = 2$ and $\epsilon_a = -2$ for $E > 0$; analogous graphs for $E < 0$ may be obtained via the symmetry condition mentioned just after equation (3.5). It is seen that all of the calculated equilibrium solutions are asymptotically stable because $r(x) > 0$ in all cases. Although these results are for the typical physical parameters stated at equation (3.6), general equilibrium solutions will produce qualitatively similar plots and results. These results greatly extend the previous results obtained when the tilt of the electric field was set to zero, i.e. $\alpha = 0$ ($c = 0$) [7].

Remark. It is apparent from figure 4 that $\mathrm{d}\phi/\mathrm{d}x$ is in general not single signed and can be zero at some point lying strictly between $x = 0$ and $x = 1$, for example, at high magnitude fields. If, however, the derivative of ϕ were non-zero and single signed on the closed interval $[0, 1]$ then the non-negativity of the eigenvalues would follow analytically by an argument similar to that contained in [21, section IIIA].

4.2. Eigenvalues and response times

We now return to equation (4.9) to determine the first (least) eigenvalue λ_1. It is known from the results presented in figure 5 that the eigenvalues must all be strictly positive. The dominant behaviour of the decaying perturbation is controlled by the magnitude of λ_1, as dictated by the form given in equation (4.5). The first eigenvalue λ_1 and its corresponding eigenfunction will be determined numerically by the standard Ritz method [22, pp 105–205] applied to equation (4.9) which, of course, is simply a reformulation of the original Sturm–Liouville problem in (4.6). Knowledge of λ_1 will then enable an estimate for the response time of perturbations to the equilibrium solutions.

The first eigenvalue λ_1 is known to be the minimum possible value of $I(v)$ when we seek a normalized function v that satisfies

$$\int_0^1 v^2(x)\,\mathrm{d}x = 1. \tag{4.15}$$

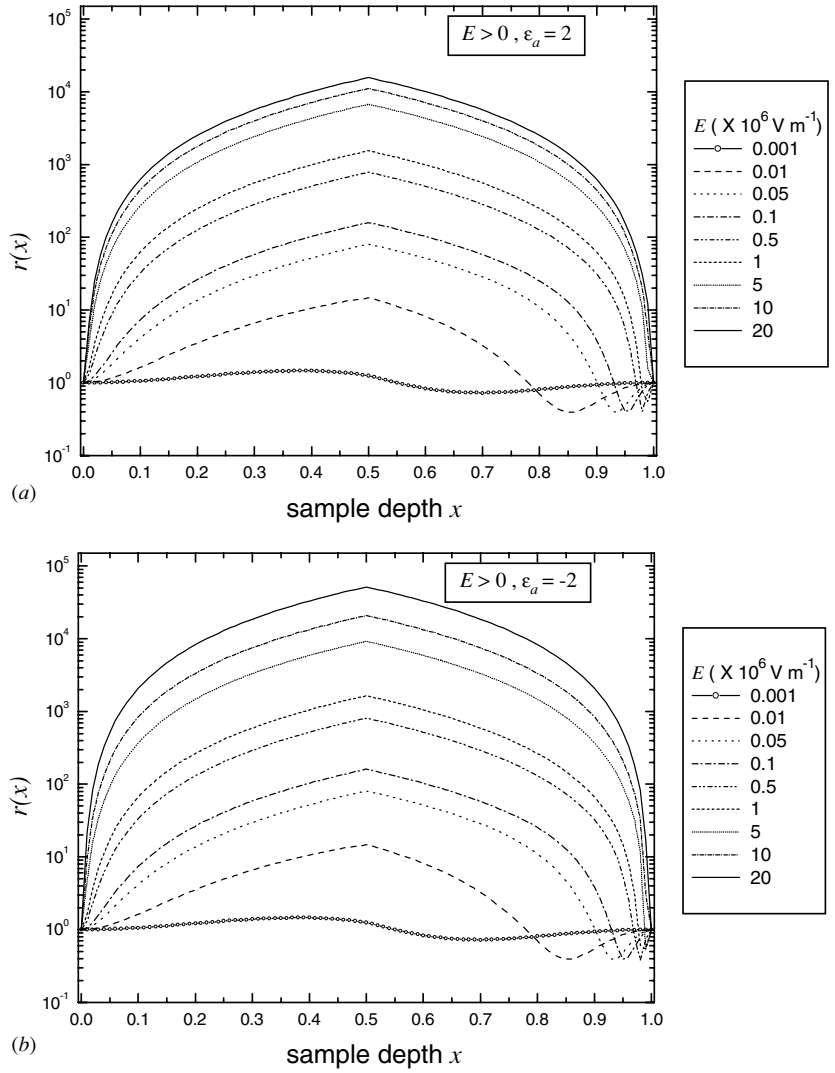

Figure 5. The positivity of the stability criterion $r(x)$ (defined by (4.14)) for $E > 0$ when (*a*) $\epsilon_a = 2$ and (*b*) $\epsilon_a = -2$ for the solutions displayed in figures 3(*a*) and 4(*a*). The solutions are asymptotically stable in all cases. Analogous graphs showing stability can be found for the case $E < 0$ via the symmetry condition mentioned after (3.5).

It is also well known [22] that the function v which delivers this minimum value λ_1 is the normalized eigenfunction corresponding to the eigenvalue λ_1 for the Sturm–Liouville problem given in form (4.9). The Ritz method allows us to approximate λ_1 and v to any required accuracy. The first step in this procedure is to select a suitable complete sequence of orthogonal functions. For our purposes it is sufficient to choose the complete sequence of functions $\{\phi_k(x)\}$, $k = 1, 2, 3, \ldots$, defined by

$$\phi_k(x) = \sin(k\pi x), \qquad k = 1, 2, 3, \ldots \tag{4.16}$$

which satisfy the orthogonality condition

$$\int_0^1 \sin(k\pi x)\sin(m\pi x)\,\mathrm{d}x = 0, \qquad k \neq m. \tag{4.17}$$

The second step is to set

$$v_n(x) = \sum_{k=1}^{n} \alpha_k \phi_k(x), \qquad n = 1, 2, 3, \ldots, \tag{4.18}$$

where $\alpha_k, k = 1, 2, 3, \ldots, n$, are constants and, for a given fixed value of n, consider the minimization of $I(v_n)$, which is now a function of the n variables α_k, with respect to the α_k subject to the constraint (4.15), which becomes

$$\int_0^1 v_n^2(x)\,\mathrm{d}x = \frac{1}{2}\sum_{k=1}^{n} \alpha_k^2 = 1. \tag{4.19}$$

Note also that $I(v_n)$ is actually a quadratic form in $\alpha_k, k = 1, 2, \ldots, n$, so that if we set $\boldsymbol{\alpha} = (\alpha_1, \alpha_2, \ldots, \alpha_n)$ then we can write

$$I(v_n) = \boldsymbol{\alpha}^T \mathbf{A}\boldsymbol{\alpha}, \tag{4.20}$$

where $\mathbf{A}$ is the unique symmetric matrix for the quadratic form. The minimization is accomplished via the Lagrange multiplier method by minimizing the function J defined by

$$J(\alpha_1, \alpha_2, \ldots, \alpha_n, \mu) = I(v_n) - \mu\left(\frac{1}{2}\sum_{k=1}^{n} \alpha_k^2 - 1\right), \tag{4.21}$$

where the constant μ is a Lagrange multiplier. This is a real-valued function of the $n + 1$ unknowns $\alpha_1, \alpha_2, \ldots, \alpha_n$ and μ. Differentiating J with respect to α_k in order to minimize it gives n equations to be satisfied in μ and the unknown components of $\boldsymbol{\alpha}$, namely, $\mathbf{A}\boldsymbol{\alpha} = (\mu/2)\boldsymbol{\alpha}$: these n equations combined with the constraint (4.19) (which guarantees that $\boldsymbol{\alpha} \neq \mathbf{0}$) give $n + 1$ equations in the $n + 1$ unknowns: moreover, it shows that $\boldsymbol{\alpha}$ is an eigenvector of the matrix $\mathbf{A}$ corresponding to its eigenvalue $\mu/2$. Solving these simultaneous equations gives values for the α_k and the Lagrange multiplier μ, which then yields the possible functions v_n via (4.18): the values of these multipliers must coincide with twice the eigenvalues $\mu/2$ of $\mathbf{A}$. The minimum value of $I(v_n)$ over functions of form (4.18) is equal to the lowest valued possibility for μ: this is because, by (4.19) and (4.20), the consequent solutions for $\boldsymbol{\alpha}$ show that

$$I(v_n) = \boldsymbol{\alpha}^T\mathbf{A}\boldsymbol{\alpha} = \frac{\mu}{2}\boldsymbol{\alpha}\cdot\boldsymbol{\alpha} = \mu. \tag{4.22}$$

Thus, since $I(v_n)$ is a quadratic form, it follows, from the theory of minimization of a quadratic form subject to the normalization constraint (4.19), that the minimum value of $I(v_n)$ is actually equal to the lowest valued Lagrange multiplier, which, in this instance, is twice the lowest eigenvalue of $\mathbf{A}$ (for a more detailed discussion on this topic see [23]). We can choose to label this value as μ_n so that $I(v_n) = \mu_n$ where the coefficients appearing in v_n are the components of the eigenvector $\boldsymbol{\alpha}$ which is connected with the Lagrange multiplier μ_n (through the least eigenvalue $\mu_n/2$ of $\mathbf{A}$). It can be shown [22] that if this procedure is repeated for each $n = 1, 2, 3, \ldots$, then the sequence of numbers $\{\mu_n\}$ is decreasing and

$$\mu_n \to \lambda_1 \qquad \text{and} \qquad v_n(x) \to v(x) \quad \text{as } n \to \infty, \tag{4.23}$$

where λ_1 and v are the first eigenvalue and its corresponding normalized eigenfunction, respectively, that we are seeking as solutions to the Sturm–Liouville problem (4.9). The constants μ_n and functions v_n act as approximations to λ_1 and v, respectively, for sufficiently large n.

The above procedure for solving the $n + 1$ equations mentioned above can be carried out numerically for $q(x)$ and $I(v)$ as defined above at equations (4.7) and (4.10) for the data

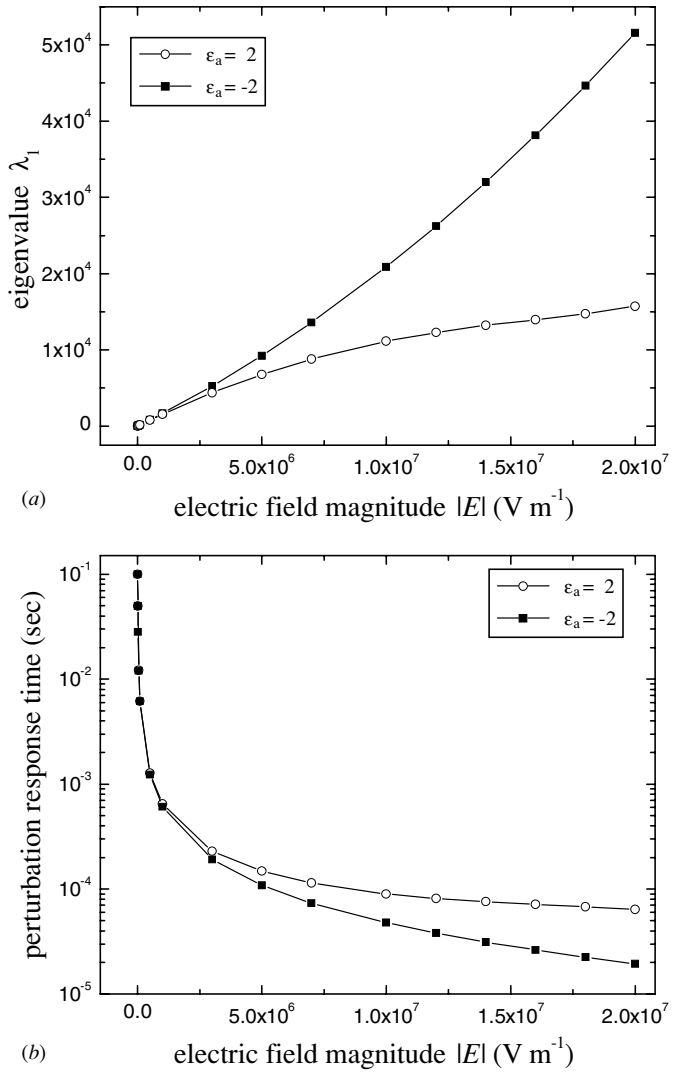

Figure 6. (*a*) The first eigenvalue λ_1 for perturbations calculated numerically by the Ritz method as outlined in the text. These values have been derived using the solutions obtained in figures 3 and 4, which assumed the one-constant approximation for the elastic constants and employed the data (3.6). The symbols represent actual values that have been calculated at given electric field magnitudes. (*b*) The perturbation response times t_r defined in equation (4.24) for $2\lambda_5 = 0.05$ Pa s with the data given by (3.6). In this particular instance $t_r = 1/\lambda_1$ where λ_1 is given in (*a*).

obtained to produce the equilibrium solutions shown in figures 3 and 4. Some numerical results are shown in figure 6(*a*), where it is seen that λ_1 increases as $|E|$ increases for either sign of ϵ_a. The response times t_r (in seconds) of the perturbations may be defined in the usual way [4] via (4.1) and (4.5) by setting $\lambda = \lambda_1$ to find

$$t_r \equiv \left(\lambda_1 \frac{T}{t}\right)^{-1} = \frac{\tau_d}{\lambda_1}. \tag{4.24}$$

In addition to the particular parameters (3.6) used throughout this paper we may take $2\lambda_5 = 0.05$ Pa s as a typical value for the viscosity [3, p 176], [4]. It then follows from (4.24)

that the response times are simply given by $t_r = 1/\lambda_1$. These response times for the perturbations are shown in figure 6(b) for the data displayed in figure 6(a).

5. Anisotropy in the elastic constants

The results presented in sections 3 and 4 were obtained under the assumption that $B_1 = B_2 \equiv B$. The analysis can essentially be repeated when $B_1 \neq B_2$ by examining equation (2.25). To simplify matters, attention will be restricted to cases where the dielectric anisotropy and the electric field are positive: we choose to set $\epsilon_a = 2$, take the electric field values 10^4, 10^6 and 10^7 V m^{-1} and adopt the material parameters listed in equation (3.6) in order to focus upon the qualitative features. Negative values for ϵ_a and other electric field magnitudes can be handled in a similar way. It proves convenient to set

$$k = \frac{B_2}{B_1}, \qquad B_1 = 5 \times 10^{-12}\ \text{N}. \tag{5.1}$$

The control parameter $k > 0$ is a measure of the anisotropy in the elastic constants and will facilitate a discussion of the influence of differing elastic constants upon the equilibrium solutions and their stability.

The time-independent equilibrium solutions to (2.25) satisfy

$$[1 + (k-1)\sin^2\phi]\frac{\mathrm{d}^2\phi}{\mathrm{d}x^2} + (k-1)\left(\frac{\mathrm{d}\phi}{\mathrm{d}x}\right)^2 \sin\phi\cos\phi = aE^2\sin\phi\cos\phi + bE\cos\phi + cE^2\sin\phi, \tag{5.2}$$

where, as in section 3, we have normalized x and the constants a, b and c are as defined in equations (3.2) to (3.4), except that B is replaced by B_1. The boundary conditions (3.5) are also retained. The solutions to (5.2) have been calculated numerically in Maple 8 and are displayed in figure 7 for the electric field magnitudes mentioned in the previous paragraph. The solutions for $k = 1$ coincide with those presented in figure 3(a) when the elastic constants are equal. Compared to the solutions obtained when the elastic constants are equal, anisotropy in the elastic constants has a more pronounced effect upon solutions at low field magnitudes.

The stability of these solutions can be investigated in the same way as described in section 4. Nevertheless, for brevity, we shall not derive an analogue of the stability criterion mentioned in section 4.1 but rather proceed directly to the calculation of eigenvalues and response times of small perturbations to the equilibrium solutions. As before, $\overline{\phi}(x)$ will denote any equilibrium solution to (5.2) and we consider a perturbation $w(x, T)$ to it of the form given via equations (4.3) and (4.5) where T is defined by (4.1) with B replaced by B_1. The dynamic equation for w can be derived from (2.25) and, in terms of the variables x and T, is given by an equation analogous to (4.4) when terms are taken to first order of magnitude in w, namely,

$$\frac{\partial w}{\partial T} = [1 + (k-1)\sin^2\overline{\phi}]\frac{\mathrm{d}^2 w}{\mathrm{d}x^2} + (k-1)\frac{\mathrm{d}\overline{\phi}}{\mathrm{d}x}\sin(2\overline{\phi})\frac{\mathrm{d}w}{\mathrm{d}x} + (k-1)\left[\left(\frac{\mathrm{d}\overline{\phi}}{\mathrm{d}x}\right)^2\cos(2\overline{\phi}) + \frac{\mathrm{d}^2\overline{\phi}}{\mathrm{d}x^2}\sin(2\overline{\phi})\right]w - [aE^2\cos(2\overline{\phi}) - bE\sin\overline{\phi} + cE^2\cos\overline{\phi}]w, \tag{5.3}$$

recalling that $\overline{\phi}(x)$ is a solution to (5.2). Since w has the supposed form (4.5), equation (5.3) and its boundary conditions can be written as

$$\frac{\mathrm{d}^2 v}{\mathrm{d}x^2} + R(x)\frac{\mathrm{d}v}{\mathrm{d}x} + \{\lambda\rho(x) - Q(x)\}v = 0, \qquad v(0) = v(1) = 0, \tag{5.4}$$

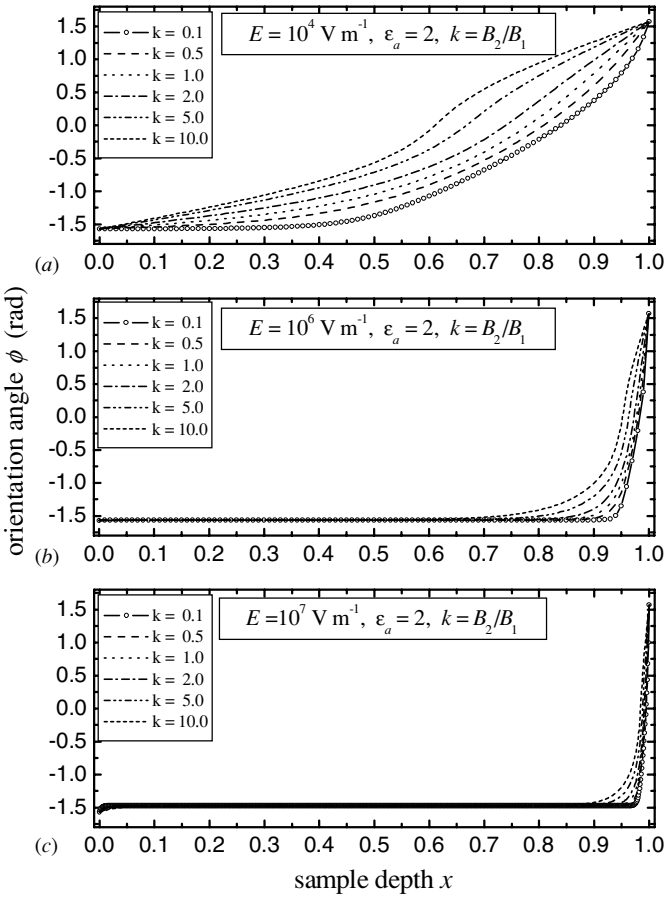

Figure 7. Numerical solutions to equation (5.2) with boundary conditions (3.5) for the parameters (3.6) when $\epsilon_a = 2$, $B_1 = 5 \times 10^{-12}$ N and $B_2 = kB_1$ where k takes the values indicated in the figures. (*a*) $E = 10^4$ V m $^{-1}$, (*b*) $E = 10^6$ V m $^{-1}$, (*c*) $E = 10^7$ V m $^{-1}$.

where

$$\rho(x) = [1 + (k-1)\sin^2\overline{\phi}]^{-1}, \tag{5.5}$$

$$R(x) = \rho(x)(k-1)\sin(2\overline{\phi})\frac{\mathrm{d}\overline{\phi}}{\mathrm{d}x}, \tag{5.6}$$

$$Q(x) = \rho(x)\left\{aE^2\cos(2\overline{\phi}) - bE\sin\overline{\phi} + cE^2\cos\overline{\phi} - (k-1)\left[\left(\frac{\mathrm{d}\overline{\phi}}{\mathrm{d}x}\right)^2\cos(2\overline{\phi}) + \frac{\mathrm{d}^2\overline{\phi}}{\mathrm{d}x^2}\sin(2\overline{\phi})\right]\right\}. \tag{5.7}$$

Note that $0 < \rho(x) < \infty$ for all $k > 0$ and all $\overline{\phi}$. Equation (5.4) can be put into normal form by introducing the transformation [24, p 394]

$$v = \tilde{v}\exp\left\{-\frac{1}{2}\int R(x)\,\mathrm{d}x\right\}, \tag{5.8}$$

which leads to

$$\frac{\mathrm{d}^2\tilde{v}}{\mathrm{d}x^2} + \{\lambda\rho(x) - q(x)\}\tilde{v} = 0, \qquad \tilde{v}(0) = \tilde{v}(1) = 0, \tag{5.9}$$

where $q(x)$ is now defined by

$$q(x) = Q(x) + \left\{\frac{1}{4}R^2 + \frac{1}{2}\frac{\mathrm{d}R}{\mathrm{d}x}\right\}. \tag{5.10}$$

Equation (5.9) can be multiplied by $\tilde{v}$ and integrated over $0 \leqslant x \leqslant 1$, with the term involving the second derivative in x integrated by parts, to find that, after applying the boundary conditions on $\tilde{v}$,

$$\int_0^1 \left[\left(\frac{\mathrm{d}\tilde{v}}{\mathrm{d}x}\right)^2 + q(x)\tilde{v}(x)^2\right]\mathrm{d}x = \lambda\int_0^1 \rho(x)\tilde{v}^2(x)\,\mathrm{d}x, \tag{5.11}$$

which is the form of a regular Sturm–Liouville problem with weight function $\rho(x)$. This is the analogue of equation (4.9) in section 4.1.

The integral $I(\tilde{v})$ can be defined as in equation (4.10) with the obvious replacement of v by $\tilde{v}$ and with q redefined by (5.10). The first eigenvalue of the above Sturm–Liouville problem is, as before, known to be the minimum of $I(\tilde{v})$ when the normalized eigenfunctions satisfy

$$\int_0^1 \rho(x)\tilde{v}^2(x)\,\mathrm{d}x = 1. \tag{5.12}$$

The Ritz method outlined in section 4.2 can be appropriately modified to cover this situation and applied again here to the numerical solutions displayed in figure 7. This procedure results in finding the first eigenvalues λ_1 for these perturbation solutions. The response times t_r are defined by equation (4.24) with B replaced by B_1 in the definition of τ_d in (4.1), which leads to, in this instance, $t_r = 1/\lambda_1$, as has arisen in the previous section. The calculated first eigenvalues and the corresponding response times for perturbations to the equilibrium solutions in figure 7 are shown in figure 8. It is seen from figure 8 that the influence of anisotropy in the elastic constants is most apparent at low magnitude electric fields, as is the case for the equilibrium solutions themselves. Note also that the results presented in figure 8 at $k = 1$ coincide with those presented in figure 7.

6. Discussion

Static solutions, and features of their stability, for the c-director in bookshelf SmC* liquid crystal under the influence of a tilted electric field in the geometry of figure 2 have been determined numerically when the one-constant approximation $B_1 = B_2 \equiv B$ has been made in sections 3 and 4 and for unequal constants in section 5. The boundary conditions on the c-director orientation angle ϕ are given by (2.28) and represent a net change of π radians in the orientation of **c** between the boundary plates. Equilibrium solutions in the one-constant approximation for various magnitudes of electric field and for different signs of the dielectric anisotropy were found numerically and displayed in figures 3 and 4 for the typical physical parameters (3.6). Similar solutions can be obtained for other boundary conditions: those stated at (2.28) were selected because many 'twisted cell' geometries in liquid crystal displays employ a relative change between the plates of $\pi/2$ or π. Stability of these equilibrium solutions in the one-constant approximation was discussed in section 4 and a stability criterion for perturbations to these solutions was established at equation (4.14). This allowed the stability to be confirmed numerically in figure 5. These results encouraged a further investigation

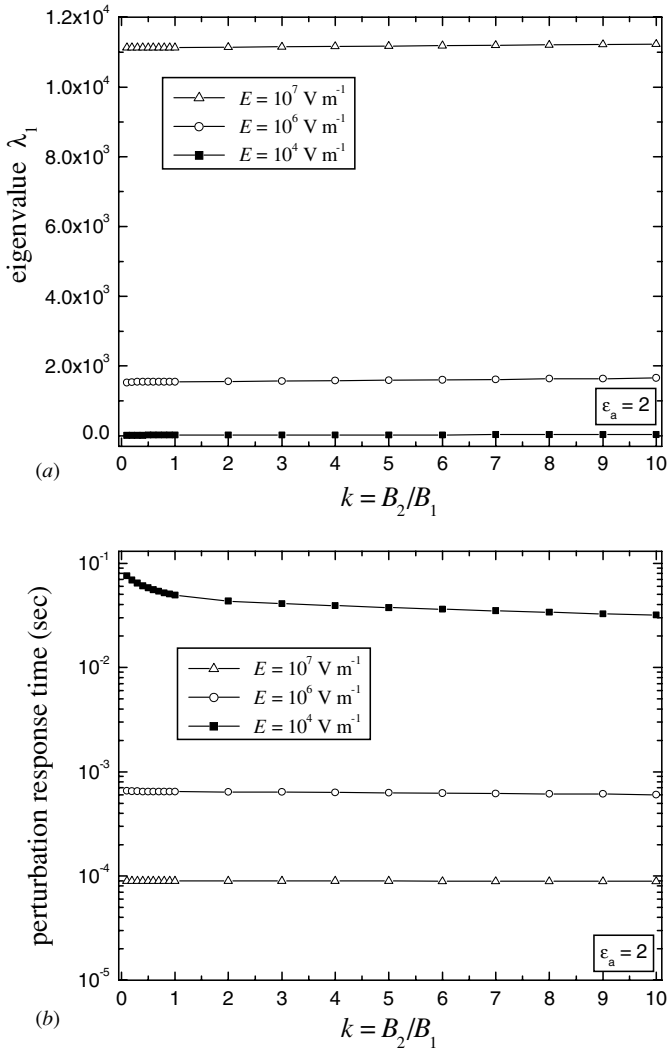

Figure 8. (*a*) The dependence of the first eigenvalue λ_1 upon the (dimensionless) anisotropy k of the elastic constants when $\epsilon_a = 2$, calculated numerically for perturbations by the Ritz method applied to equation (5.11) using solutions obtained in figure 7, as discussed in the text. (*b*) The perturbation response times t_r defined in equation (4.24) with B set equal to B_1 in (5.1), $d = 10\,\mu$m and $2\lambda_5 = 0.05$ Pa s; $t_r = 1/\lambda_1$ for these data where λ_1 is given in (*a*).

in section 4.2 into the asymptotic decay in time of small perturbations to the equilibrium solutions via a Sturm–Liouville problem using the Ritz method. The first eigenvalue for the perturbation v was calculated numerically for each of the equilibrium solutions obtained earlier: the results appear in figure 6(*a*). This enabled the determination of the response times, shown in figure 6(*b*), for such perturbations for a typical tilted field angle ($\alpha = 5^\circ$), a feature that has physical significance but was not considered in related earlier work [7]. The results will be qualitatively similar for physical data other than those given by (3.6) and therefore they can be generalized to a wider range of cases by analogous calculations.

It should be mentioned that the equation considered by Anderson and Stewart [7] may be recovered from equation (3.1) by setting $\alpha = 0$ and replacing ϕ by $\phi + \pi/2$; although

this transformation gives mathematically the same form of equation discussed in [7], different boundary conditions were applied in a different geometry which forced a reorientation of **c** in the z direction perpendicular to the smectic layers with the only elastic constant being B_3, which would take the rôle of B in section 3 above. The analysis presented here remains valid at $\alpha = 0$ (when the electric field is no longer tilted relative to the smectic layers) and so the results extend those in [7].

The anisotropy k in the elastic constants was considered in section 5. Despite the equilibrium equation being more complex, stability results for equilibrium solutions were established by calculations similar to those carried out in sections 3 and 4. This was achieved after a reformulation of the governing equation led to equation (5.11) and an application of the Ritz method for the identification of the first eigenvalue for a perturbation to each solution. For brevity, only the case for $\epsilon_a = 2$ was discussed, with typical solutions being shown in figure 7: $k = 1$ corresponds to the one-constant approximation $B_1 = B_2$ that was assumed in sections 3 and 4. The dependence upon k of the corresponding eigenvalues and response times for perturbations is shown in figure 8 for the indicated field magnitudes and material parameters. Other choices of parameters will lead to similar qualitative results.

The results in this paper are for samples that are finite in the x direction. In such circumstances the c-director orientation angle ϕ is different on each boundary and smooth constant equilibrium solutions are therefore not possible. The applied electric field forces the director to adjust and attempts to achieve its preferred optimum constant equilibrium state via a competition between the boundary conditions and its idealized state in the bulk. Consequently, the spatially dependent equilibrium solution biases itself towards its preferred alignment in as much of the bulk of the cell as possible, especially at high magnitude fields. This behaviour is apparent from the results presented in figures 3, 4 and 7 where it is evident that for high magnitude fields the solution $\phi(x)$ is almost constant across most of the central part of the sample. These constant states can be identified by considering the idealized case of an infinite sample: they are the minima of w_{elec} in (2.6) as a function of ϕ. These constant equilibrium states have been considered in detail by Stewart and Momoniat [16] in cases corresponding to $\alpha \geqslant 0$ and by Anderson and Stewart [6] when $\alpha = 0$.

It is worth noting that the techniques employed here may be capable of being adapted to those for a sample of SmC* liquid crystal in which the smectic layers are themselves tilted relative to the boundary plates while the electric field is not tilted to the plates, a situation that has been considered previously by Schiller *et al* [25] in the context of domain walls moving parallel to the plates. Related work on tilted layers of SmC* may also be found in the articles by Abdulhalim *et al* [8, 9].

Throughout this paper it has been assumed that flow, particularly backflow (see [4] for details), can be neglected, an assumption that is feasible because the field is neither suddenly switched on nor switched off. This is common practice in simplified versions of theoretical work in liquid crystals and it would be natural to extend our investigation by seeking solutions to this problem when flow is present using the dynamic theory for smectics [11, 4], especially when a high magnitude field is suddenly switched off. Some related preliminary work on relaxation incorporating flow as the electric field is switched off has been reported [26] for SmC in the bookshelf geometry with the differing boundary conditions (2.28) and it is expected that work on SmC* may proceed in a similar manner. Backflow for SmC in the bookshelf geometry with $\phi = 0$ at both boundaries has been investigated in detail by Blake and Leslie [27] while Blake *et al* [28] have examined backflow for SmC* in the bookshelf geometry for symmetric and asymmetric boundary conditions. For a more extensive physical discussion of backflow for SmC* in the bookshelf geometry, and some examples of numerical solutions, the reader should consult the work by Zhong Zou *et al* [29]. The work in this paper should

lend motivation for further more intricate investigations into the influence of backflow upon director reorientation in SmC*, a topic that will be of interest to the modelling of switching in SmC* displays, especially since it is known that backflow can, in certain geometries, be significantly influential in the switching process of nematic liquid crystal displays [4, 30–32].

References

[1] de Gennes P G and Prost J 1993 *The Physics of Liquid Crystals* 2nd edn (Oxford: Clarendon)
[2] Lagerwall S T and Dahl I 1984 *Mol. Cryst. Liq. Cryst.* **114** 151–87
[3] Lagerwall S T 1999 *Ferroelectric and Antiferroelectric Liquid Crystals* (Weinheim: Wiley-VCH)
[4] Stewart I W 2004 *The Static and Dynamic Continuum Theory of Liquid Crystals* (London and New York: Taylor and Francis)
[5] Maclennan J E, Clark N A and Handschy M A 1992 Solitary waves in ferroelectric liquid crystals *Solitons in Liquid Crystals* ed L Lam and J Prost (New York: Springer) pp 151–90
[6] Anderson D A and Stewart I W 2000 *Phys. Rev.* E **62** 5043–55
[7] Anderson D A and Stewart I W 2001 *Int. J. Eng. Sci.* **39** 1191–215
[8] Abdulhalim I, Moddel G and Clark N A 1992 *Appl. Phys. Lett.* **60** 551–3
[9] Abdulhalim I, Moddel G and Clark N A 1994 *J. Appl. Phys.* **76** 820–31
[10] Clark N A and Lagerwall S T 1980 *Appl. Phys. Lett.* **36** 899–901
[11] Leslie F M, Stewart I W and Nakagawa M 1991 *Mol. Cryst. Liq. Cryst.* **198** 443–54
[12] Oseen C W 1933 *Trans. Faraday Soc.* **29** 883–99
[13] Leslie F M, Stewart I W, Carlsson T and Nakagawa M 1991 *Continuum Mech. Thermodyn.* **3** 237–50
[14] Carlsson T, Stewart I W and Leslie F M 1992 *J. Phys. A: Math. Gen.* **25** 2371–4
[15] Carlsson T, Stewart I W and Leslie F M 1991 *Liq. Cryst.* **9** 661–78
[16] Stewart I W and Momoniat E 2004 *Phys. Rev.* E **69** 061714
[17] Dunmur D A, Fukuda A and Luckhurst G R (ed) 2001 *Physical Properties of Liquid Crystals: Nematics (EMIS Datareviews Series No 25)* The Institution of Electrical Engineers (London: INSPEC)
[18] Maple 8 2002 (Waterloo, Canada: Maplesoft)
[19] Troutman J L 1994 *Boundary Value Problems of Applied Mathematics* (Boston, MA: PWS Publishing)
[20] Davies E B 1995 *Spectral Theory and Differential Operators* (Cambridge: Cambridge University Press)
[21] Stewart I W 1998 *Phys. Rev.* E **57** 5626–33
[22] Gelfand I M and Fomin S V 2000 *Calculus of Variations* (New York: Dover) (Revised English edition)
[23] Kaplan W 1984 *Advanced Calculus* 3rd edn (Menlo Park, CA: Addison–Wesley)
[24] Ince E L 1956 *Ordinary Differential Equations* (New York: Dover)
[25] Schiller P, Pelzl G and Demus D 1987 *Liq. Cryst.* **2** 21–30
[26] Woods P D, Stewart I W and Mottram N J 2004 *Mol. Cryst. Liq. Cryst.* **413** 271–8
[27] Blake G I and Leslie F M 1998 *Liq. Cryst.* **25** 319–27
[28] Blake G I, Leslie F M and Towler M J 1997 *Eur. J. Appl. Math.* **8** 263–71
[29] Zhong Zou, Clark N A and Carlsson T 1994 *Phys. Rev.* E **49** 3021–30
[30] Gerritsma C J, van Doorn C Z and van Zanten P 1974 *Phys. Lett.* A **48** 263–4
[31] Clark M G and Leslie F M 1978 *Proc. R. Soc. Lond.* A **361** 463–85
[32] Sambles J R and Ruan L Z 2004 *J. Non-Newtonian Fluid Mech.* **119** 39–49